

SCIENTIFIC REPORTS



OPEN

Effects of elevated CO₂ on phytoplankton during a mesocosm experiment in the southern eutrophicated coastal water of China

Xin Liu¹, Yan Li¹, Yaping Wu¹, Bangqin Huang¹, Minhan Dai¹, Feixue Fu², David A. Hutchins² & Kunshan Gao¹

There is a growing consensus that the ongoing increase in atmospheric CO₂ level will lead to a variety of effects on marine phytoplankton and ecosystems. However, the effects of CO₂ enrichment on eutrophic coastal waters are still unclear, as are the complex mechanisms coupled to the development of eutrophication. Here, we report the first mesocosm CO₂ perturbation study in a eutrophic subtropical bay during summer by investigating the effect of rising CO₂ on a model artificial community consisting of well-characterized cultured diatoms (*Phaeodactylum tricornutum* and *Thalassiosira weissflogii*) and prymnesiophytes (*Emiliania huxleyi* and *Gephyrocapsa oceanica*). These species were inoculated into triplicate 4 m³ enclosures with equivalent chlorophyll *a* (Chl-*a*) under present and higher partial pressures of atmospheric CO₂ ($p\text{CO}_2 = 400$ and 1000 ppmv). Diatom bloom events were observed in all enclosures, with enhanced organic carbon production and Chl-*a* concentrations under high CO₂ treatments. Relative to the low CO₂ treatments, the consumption of the dissolved inorganic nitrogen and uptake ratios of N/P and N/Si increased significantly during the bloom. These observed responses suggest more extensive and complex effects of higher CO₂ concentrations on phytoplankton communities in coastal eutrophic environments.

At present, one of the most far-reaching global perturbations of the marine environment is caused by the massive invasion of fossil fuel CO₂ into the ocean, making it the second largest sink for anthropogenic carbon dioxide after the atmosphere itself¹. CO₂ dissolved in seawater forms free H⁺ ions, lowering ocean pH and shifting dissolved inorganic carbon away from carbonate (CO₃²⁻) towards more bicarbonate (HCO₃⁻) and CO₂. This global effect of anthropogenic CO₂ emissions on ocean carbonate chemistry is of concern because it is already lowering the pH of the oceans, which may have ramifications for the growth, productivity and dominance of individual organisms or whole marine ecosystems².

It has been suggested that the consequences of global ocean acidification will become more acute in the coastal zone, due to the decomposition of organic matter produced in eutrophic waters³. Coastal areas are complex and dynamic places in which environmental factors typically exhibit great spatial and temporal variability. For example, CO₂ partial pressures ($p\text{CO}_2$) in the inner estuary of the highly eutrophic Pearl River was found to range from 3380 to 4785 μatm in the summer, with a pH of 7.0–7.2⁴. Meanwhile, in a concurrent bloom in the outer estuary of the Pearl River $p\text{CO}_2$ dropped rapidly to ~ 200 μatm , and pH rose to as high as 8.6⁵. This is mainly due to a variety of biogeochemical processes in coastal water, not from changes of CO₂ in atmospheric concentrations. Terrigenous inputs, upwelling effects and biological activities (algal blooms, bacterial respiration) play important roles on the variations of $p\text{CO}_2$ and pH in the water. The coastal acidification has been predicted to be over 10%

¹State Key Laboratory of Marine Environmental Science, Xiamen University, 361005, Xiamen, Fujian, China.

²Department of Biological Sciences, University of Southern California, 3616 Trousdale Parkway, Los Angeles, California, 90089, USA. Xin Liu, Yan Li and Yaping Wu contributed equally to this work. Correspondence and requests for materials should be addressed to B.H. (email: bqhuang@xmu.edu.cn) or M.D. (email: mdai@xmu.edu.cn) or K.G. (email: ksgao@xmu.edu.cn)

faster compared to pelagic waters, as the decomposition of organic carbon by bacteria leads to an extra increase in CO₂ concentration, usually associated with the processes of phytoplankton blooms and hypoxia in estuaries during summer³. Thus, although the partial pressure of CO₂ in some stages of eutrophication is lower than the anthropogenically-influenced atmospheric pCO₂, eutrophic coastal waters will still be under the influence of high pCO₂ in the future³.

Efforts to understand potential consequences and feedbacks of increasing CO₂ have been employed using both laboratory and mesocosm studies over scales ranging from genetic to ecosystem levels^{6,7}. Among the laboratory tests to investigate biological responses to ocean acidification, diazotrophic cyanobacteria, diatoms and prymnesiophytes (coccolithophores) are the most studied groups^{8,9}. In eutrophic coastal waters, diatoms and prymnesiophytes are dominant groups⁸, and responsible for a large fraction of oceanic primary production, playing an important role in marine ecosystems. Some typical species, such as *Phaeodactylum tricornutum* and *Emiliania huxleyi*, have been intensively studied with respect to their modes of C acquisition and various responses to changes in seawater CO₂ at physiological, biochemical and molecular levels^{2,10}. However, since a majority of laboratory studies have investigated responses of single species, the knowledge obtained is difficult to extrapolate to these species' responses to ocean acidification in natural complex environments. On the other hand, there are too many species in natural communities, including phytoplankton, zooplankton, and bacteria. In addition, natural communities in coastal waters have to confront to the complex influences of both natural change and human activities². Therefore, we presently know little about how these organism responses scale up to the community and ecosystem levels and what the consequences are for marine food webs and biogeochemical cycles^{6,7,11}. One way to bridge this gap between single species studies and highly complex natural communities is to test the mechanistic effects of global change factors on relatively less complex artificial communities composed of a few key phytoplankton groups¹².

Mesocosm approaches are useful to shorten this gap between laboratory tests and *in-situ* investigations, and mixtures of well-studied phytoplankton species should be studied at mesocosm level to evaluate competition and succession under elevated CO₂. Laboratory cultures are normally kept under stable conditions (e.g. constant light, temperature), while mesocosm enclosures are exposed to varying or fluctuating environmental factors, such as solar radiation and diel changes of temperature. Therefore, mesocosm enclosures are designed to approximate natural conditions in which environmental factors can be manipulated and closely monitored, and so provide a powerful tool to understand and forecast the effects of environmental changes on pelagic communities and the associated impacts on biogeochemical cycling⁶. In spite of this, recent findings show that there are still many unanswered questions using these approaches⁷. For example in mesocosm enclosures in the southern Norway, the inferred cumulative C:N stoichiometry of organic production increased with CO₂ treatments at initial CO₂ partial pressures of 350, 700 and 1,050 ppmv from 6.3 to 7.1 to 8.3 at the height of the bloom, respectively⁹. This suggests that ocean acidification may modify the stoichiometry of pelagic primary production which consumed up to 39% more dissolved inorganic carbon at increased pCO₂ compared to the ambient level, whereas nutrient draw-down remained similar^{1,9}. However, considerable uncertainty about this finding was shown in other mesocosm tests (Table S1). During a CO₂ perturbation study in Kongsfjorden on the west coast of Spitsbergen (Norway), carbon to nutrient uptake ratios were lower or higher than Redfield proportions during different phases of the experiment¹³. Another mesocosm study in the coastal waters of Korea also found the stoichiometry of elemental assimilation was insensitive to increasing pCO₂ concentration and was close to the Redfield ratio of ~6.6^{14,15}. In addition, effects of ocean acidification on phytoplankton uptake stoichiometry in coastal waters may result in a series of complicated changes in biogeochemical cycles¹⁰, such as altering the potential for phytoplankton growth limitation by nutrient elements such as P or Si over different spatial and temporal scales. Therefore, in highly productive coastal ecosystems, which support fisheries and other ecosystem services, unpredictable effects of ocean acidification ought to be intensively studied, since the biogeochemical response to increasing CO₂ is obviously more complex than has been suggested from previous studies^{7,10,13,16}.

Under eutrophic conditions, nutrient limitation of phytoplankton growth could be alleviated and CO₂ might be a limiting factor, especially during algal blooms. Subsequently, it is reasonable to hypothesize that growth of phytoplankton in eutrophic waters could be enhanced under elevated CO₂ levels. In this study, we conducted a mesocosm CO₂ perturbation study in a eutrophic subtropical bay in China during early summer, to investigate the effect of rising CO₂ on a model phytoplankton community consisting of four well-studied phytoplankton isolates. These results are then used to discuss the following questions: i) What is the effect of high CO₂ partial pressure on the growth of phytoplankton in eutrophic coastal waters? ii) How does elevated CO₂ affect the competition between diatoms and prymnesiophytes (coccolithophores), the two most studied taxonomic groups in response to ocean acidification? and iii) Will the effects of high pCO₂ on phytoplankton uptake stoichiometry in coastal waters alter the potential for limitation by nutrients such as N, P, or Si?

Results

Temporal evolution of the carbon dioxide system. The vertical variations on temperature and salinity in the enclosures were less than 0.1 °C and 0.1, respectively, indicating that the water was well mixed (Fig. S2). During the 15 days, there was a clear increase in temperature (mean value increase 2 °C) but only a slight increase in salinity (mean value increase 0.1). The initial dissolved inorganic carbon (DIC), total alkalinity (TA) and pH in the water were 2036 ± 9 (mean ± SD, the same below), 1907 ± 8 μmol kg⁻¹ and 7.75 ± 0.01, respectively (Fig. 1). Consequently, the initial pCO₂ in the water was 805 ± 22 μatm (Fig. 2a), indicating it was in fact already influenced by acidification, with a low pH and quite high DIC (Fig. 1). As expected, the initial concentrations of dissolved organic carbon (DOC) were quite high (day 1, 227 ± 15 μM).

Gradually with aeration from the CO₂ enrichers (400 and 1000 ppmv, HC and LC), there were significant differences between high and low CO₂ treatments in pH, DIC and pCO₂ in the water in the first 4 days (Fig. 2b, all

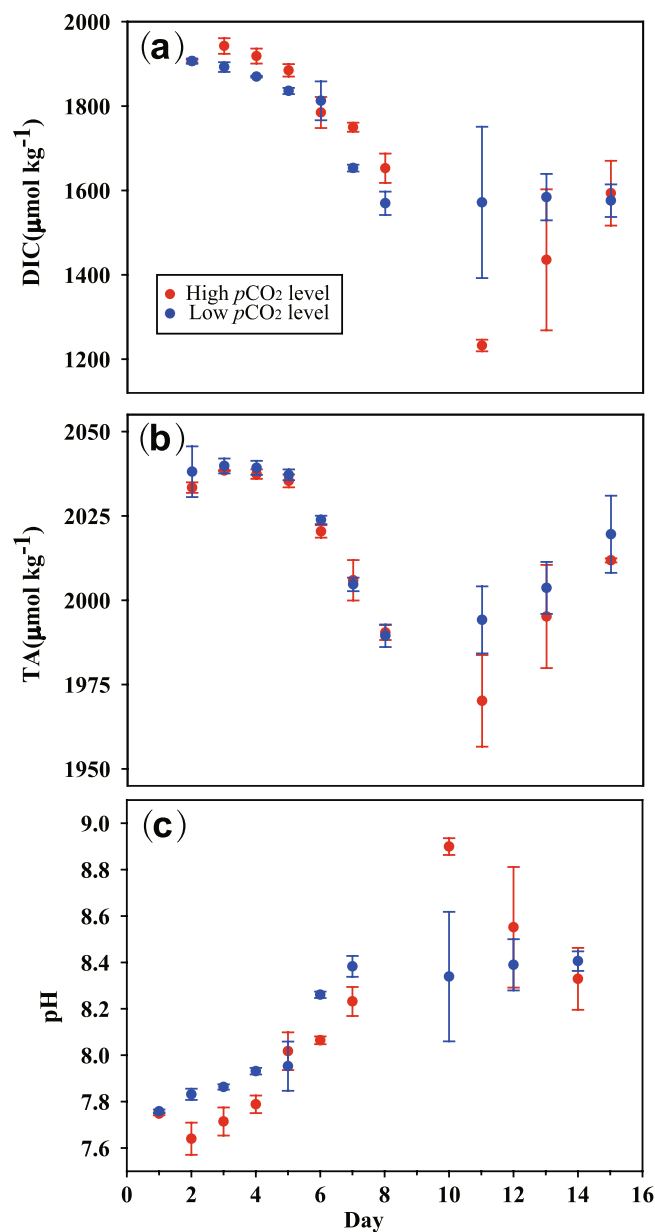


Figure 1. Temporal variations of concentrations of dissolved inorganic carbon (DIC, panel a), total alkalinity (TA, b) and pH (c) in 6 enclosures perturbed by bubbling with ambient air (400 ppmv CO₂, Low CO₂ level) or an air/CO₂ mixture at a concentration of 1000 ppmv CO₂ (High CO₂ level) over a two week incubation. Symbols are the means and error bars are the standard errors of three replicate enclosures.

$p < 0.05$). The mean $p\text{CO}_2$ levels in the HC and LC treatments were 879.15 ± 145.76 and 658.05 ± 113.98 ppmv, with a significant differences of 221.10 ppmv in the first 4 days (Fig. 2b).

Along with the growth of phytoplankton and consequent depletion of nutrients, pH value increased in all enclosures (Fig. 1c). The $p\text{CO}_2$ values dropped rapidly to $\sim 200 \mu\text{atm}$, and pH rose to over 8.5, indicating the impact of biological activity was first order. During the growth of phytoplankton, they were aerated continuously by different CO₂ enrichments. Although lower pH values and higher $p\text{CO}_2$ in the early phase were observed, quite high pH values (8.90 ± 0.06) and low $p\text{CO}_2$ ($31 \pm 2 \mu\text{atm}$) in the HC enclosures were observed on day 10 (Fig. 1).

Temporal evolution of nutrients. The initial filtered bay water used for the experiment was highly eutrophic, with nutrient concentrations in the initial waters of 30.48 ± 0.29 , 53.32 ± 1.10 , 3.42 ± 0.05 and $45.92 \pm 0.39 \mu\text{M}$ for $\text{NO}_3^- + \text{NO}_2^-$ (NO_x), NH_4^+ , PO_4^{3-} and SiO_3^{2-} , respectively (Figs 3 and 4). The composition of the dissolved inorganic nitrogen pool (DIN, $\text{NO}_x + \text{NH}_4^+$) indicates a very high proportion of NH_4^+ (Fig. 3). DIN concentrations dropped sharply after day 3 due to phytoplankton uptake, and the final drawdown in the HC treatment was significantly larger than that of the LC treatment (Fig. 3a, $p < 0.01$). Early in the nitrogen uptake process the preferential uptake of NH_4^+ is obvious, as the decrease of NO_x started only when NH_4^+ reached a

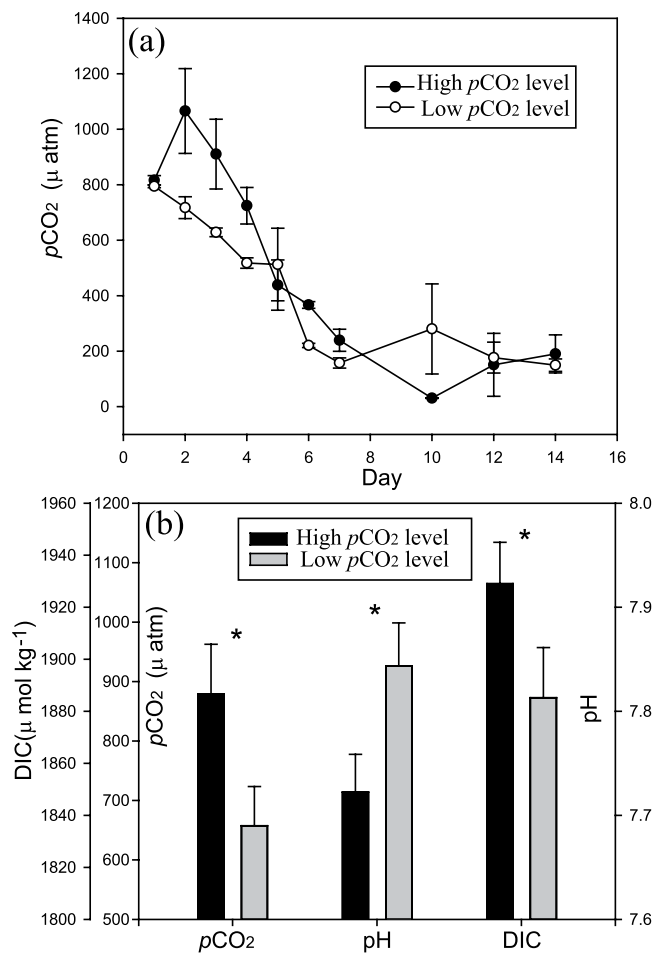


Figure 2. Temporal variations of the CO_2 partial pressure in the seawater ($p\text{CO}_2$, μatm , panel a) in 6 enclosures perturbed by bubbling with ambient air (400 ppmv CO_2 , Low CO_2 level) or an air/ CO_2 mixture at a concentration of 1000 ppmv CO_2 (High CO_2 level) over a two week incubation, and comparisons on $p\text{CO}_2$, pH and dissolved inorganic carbon (DIC) in the first 4 days (b). Symbols are the means and error bars are the standard errors of three replicate enclosures. Asterisk (*) indicate there are significant differences between enclosures ($p < 0.05$).

minimum on day 7 (Fig. 3b). The DIN drawdown difference between treatments was due to the fact that the NO_x was not exhausted under the LC scenario (Fig. 3c).

The downward trends of SRP (soluble reactive phosphate) and SiO_3^{2-} concentrations were consistent with that of ammonium, and the SRP concentrations were consumed completely first in LC treatments by day 6 (Fig. 4). Despite the eutrophic status of the collected experimental water, it was also potentially P-limited, as the SRP was first exhausted by day 6 and the initial DIN/SRP ratio was 24.5. This ratio exhibited a sustained increase along with the decline of inorganic nutrient concentrations in the seawater (Fig. 4c). Since more NO_x was used in the HC enclosures, the DIN/SRP ratios in HC treatments after day 6 were significantly lower than those of the LC enclosures. Similar results were observed for variations in the DIN/ SiO_3^{2-} ratios (Fig. 4d). Ratios of net nutrient uptake (the difference with initial concentrations) also indicated treatment-dependent differences with significantly higher ratios of $\Delta\text{DIN}/\Delta\text{SRP}$ and $\Delta\text{DIN}/\Delta\text{SiO}_3^{2-}$ in HC enclosures during the nutrient replete period (Fig. 5, day 4–7, $n = 4$, paired t-Test, $p < 0.01$). This suggests more consumption of DIN in the HC enclosures relative to SRP and SiO_3^{2-} .

Variations on phytoplankton communities and carbon metabolism. During the experiment, algal blooms were induced artificially in the enclosures (Fig. 6a). As there were no zooplankton grazers present, phytoplankton responses to the high CO_2 treatments were strictly driven by “bottom-up” influences. Although the initial total chlorophyll *a* (Chl-*a*) concentrations of the four phytoplankton species were the same and the initial cell number of the prymnesiophytes was higher than that of the diatoms, the diatoms had an obvious advantage in the highly eutrophic water (Fig. 6). This is evident from the observation that the consumption of SiO_3^{2-} was coupled to that of the other nutrients (Figs 3 and 4), as well as the increase in the diagnostic diatom pigment (Fucoxanthin, Fuco) (Fig. 6b).

Phytoplankton Chl-*a* biomass reached a significantly higher concentration in the HC treatment on day 9 ($185 \pm 59 \mu\text{g L}^{-1}$), although its response seemed to show a short time lag (Fig. 6a). Prymnesiophytes rapidly

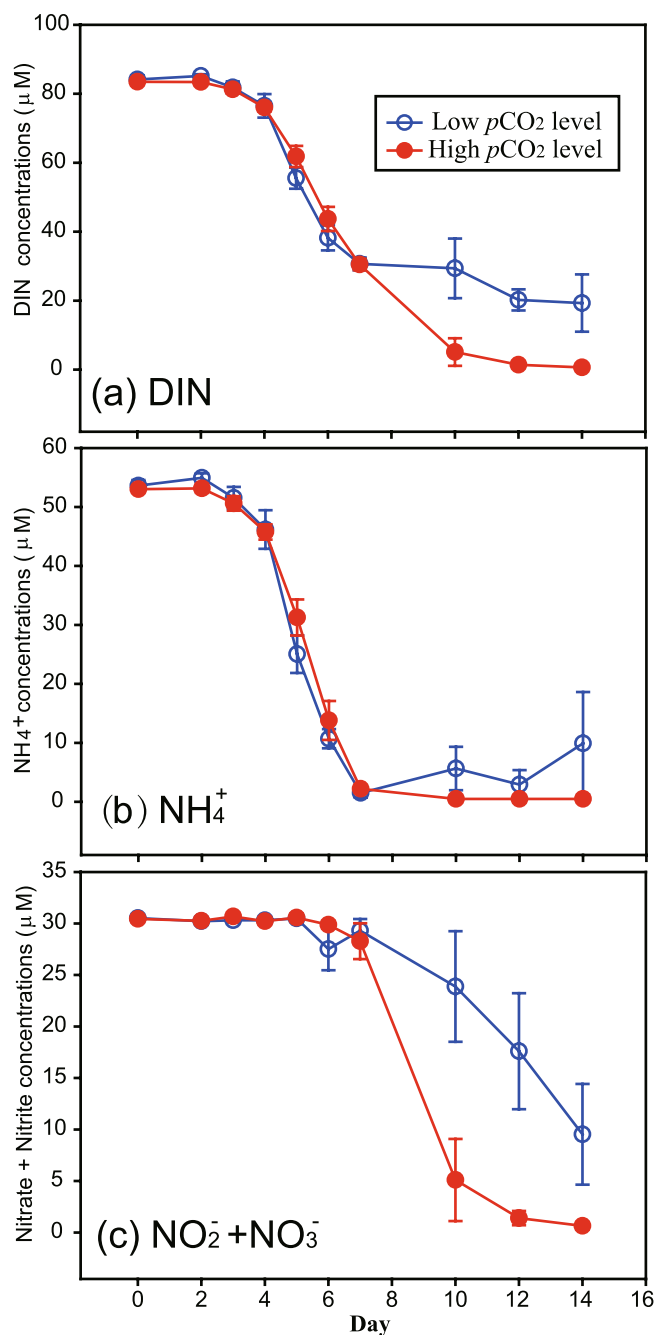


Figure 3. Temporal variations of concentrations of total dissolved inorganic nitrogen (DIN, panel a), NH_4^+ (b) and Nitrite + Nitrate (c) in 6 enclosures which were perturbed by bubbling with ambient air (400 ppmv CO_2 , Low CO_2 level) or an air/ CO_2 mixture at a concentration of 1000 ppmv CO_2 (High CO_2 level). Symbols are the means and error bars are the standard errors of three replicate enclosures.

responded in the HC enclosures as indicated by their diagnostic pigment 19'hexanoyl-oxy-fucoxanthin (19-Hex), reaching a peak on day 6 ($1.4 \pm 0.5 \mu\text{g L}^{-1}$, Fig. 6c). The temporal variations in the ratio of 19-Hex to Chl-*a* confirm that the contribution of prymnesiophytes to total Chl-*a* biomass was higher in the HC enclosures in the early phase (day 2–7), and the opposite was observed during days 8–14 (Fig. 7b). The ratios of Fuco to Chl-*a* exhibited no clear differences between the different treatments, both with a rising trend following a decline during the first few days (Fig. 7a). Based on the pigment ratios obtained in the mono-culture, the maximum Chl-*a* concentrations of diatom and prymnesiophytes in the HC enclosures were 166 ± 62 and $21 \pm 33 \mu\text{g L}^{-1}$, while they were 76 ± 6 and $5.5 \pm 3.5 \mu\text{g L}^{-1}$ in the LC treatments.

The production of CaCO_3 (calcification) by prymnesiophytes in the HC enclosures ($1.27 \pm 0.07 \mu\text{mol kg}^{-1} \text{d}^{-1}$) was significantly lower than in the LC treatment ($1.58 \pm 0.12 \mu\text{mol kg}^{-1} \text{d}^{-1}$), while the production of particulate and dissolved organic carbon (POC and DOC) showed opposite trends (Table 1). These values in the HC enclosures (20.2 ± 7.6 and $29.7 \pm 3.4 \mu\text{M d}^{-1}$, respectively) were significantly higher than those in the LC condition

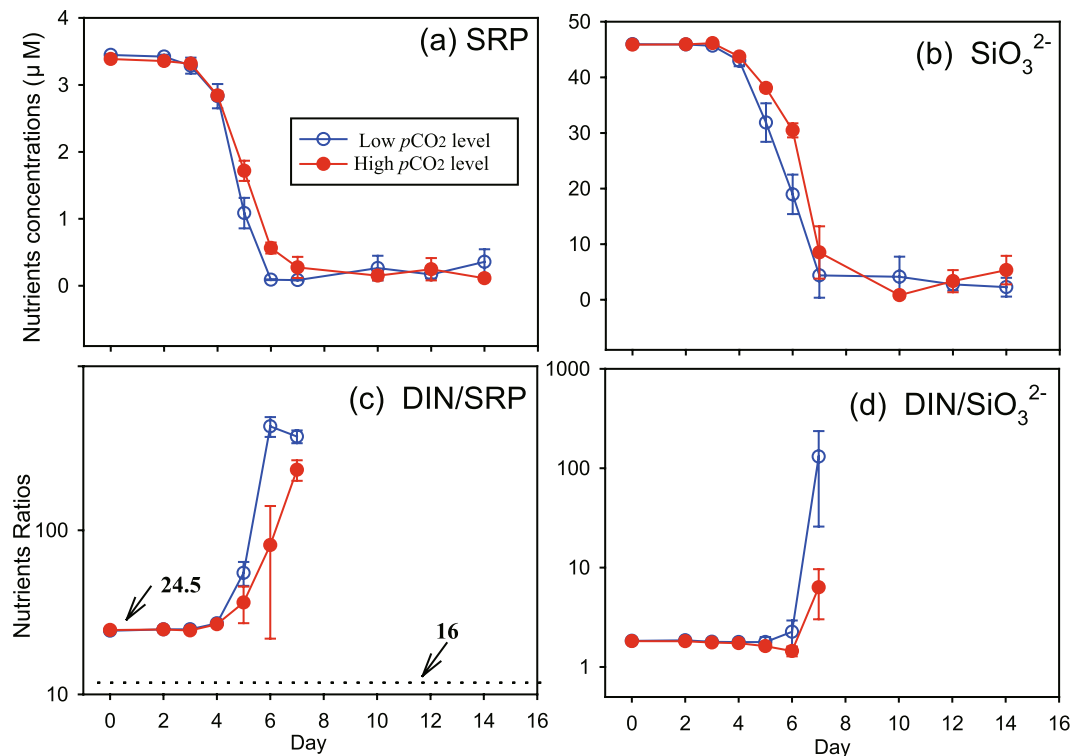


Figure 4. Temporal variations of concentrations of soluble reactive phosphorus (SRP, panel a), dissolved silicate, SiO_3^{2-} (b), and ratios of dissolved inorganic nitrogen to soluble reactive phosphorus (c, DIN/SRP) and to SiO_3^{2-} (d, DIN/ SiO_3^{2-}) in 6 seawater enclosures which were perturbed by bubbling with ambient air (400 ppmv CO_2 , Low CO_2 level) or an air/ CO_2 mixture at a concentration of 1000 ppmv CO_2 (High CO_2 level). Symbols are the means and error bars are the standard errors of three replicate enclosures. Nutrients ratio are shown during the nutrients replete period (day 0–7).

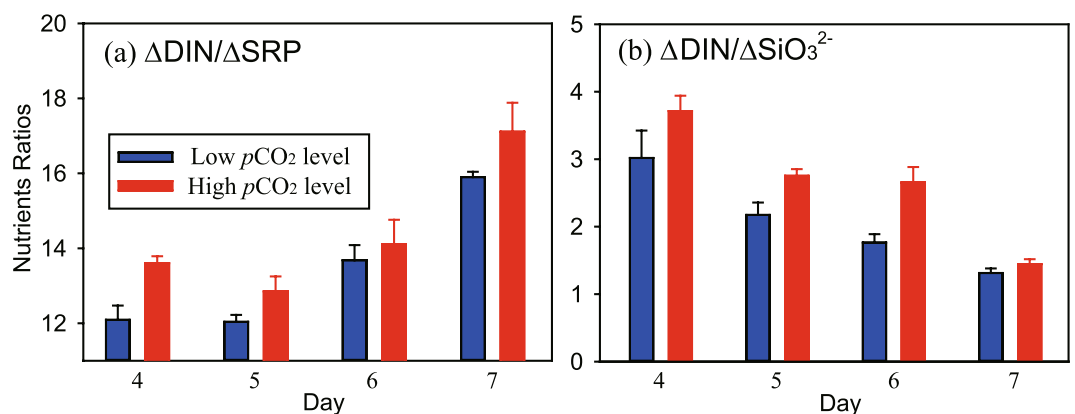


Figure 5. Temporal variations in nutrient consumption ratios of dissolved inorganic nitrogen to soluble reactive phosphorus (a, $\Delta\text{DIN}/\Delta\text{SRP}$) and to SiO_3^{2-} (b, $\Delta\text{DIN}/\Delta\text{SiO}_3^{2-}$) during the nutrients replete period (day 4–7) in 6 seawater enclosures which were perturbed by bubbling with ambient air (400 ppmv CO_2 , Low CO_2 level) or an air/ CO_2 mixture at a concentration of 1000 ppmv CO_2 (High CO_2 level). Columns are the means and error bars are the standard errors of three replicate enclosures.

(8.8 ± 4.0 and $14.2 \pm 4.8 \mu\text{M d}^{-1}$), respectively ($p < 0.01$). Thus, the ratios of particulate inorganic carbon (PIC) to POC in the HC enclosures were lower than those in the LC enclosures (Table 1).

Discussion

Enhanced biomass and production under HC treatment. As we mentioned above, acidification in eutrophic waters is not only accompanied by but also coupled to the development of eutrophication³. In natural sea water, typically the DOC concentration is less than $100 \mu\text{M}$, and a least half of which is resistant to biological

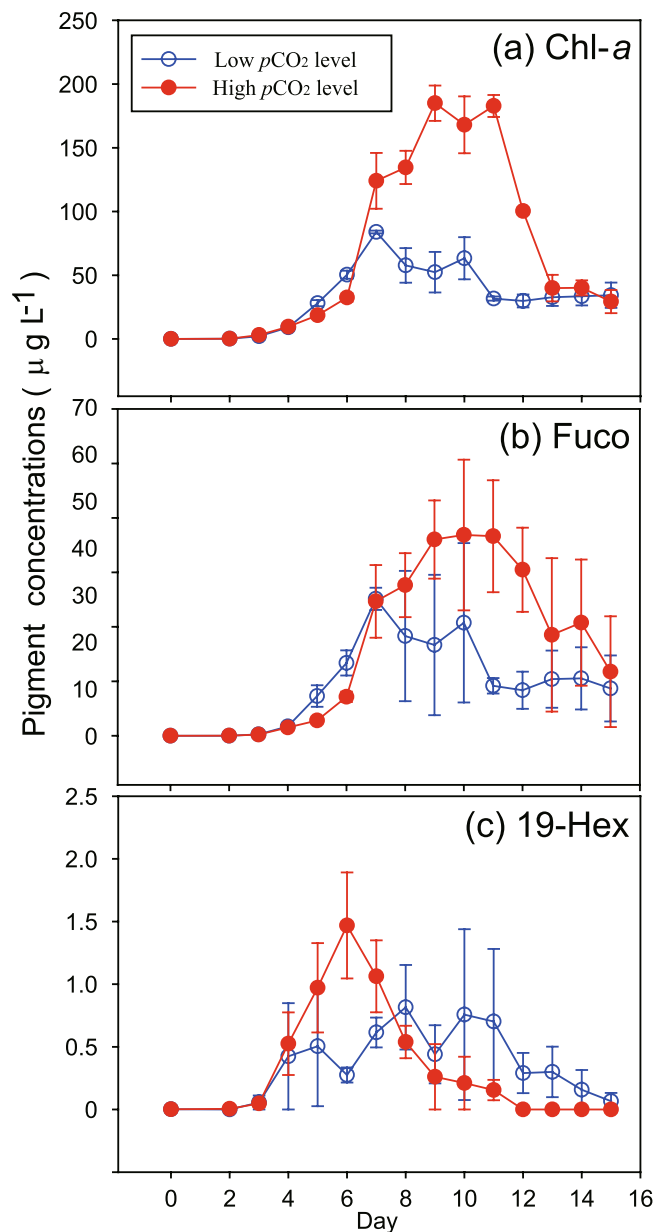


Figure 6. Temporal variations in concentrations of chlorophyll *a* (a) and diagnostic pigments of diatoms (b, Fucoxanthin) and prymnesiophytes (c, 19′hexanoyl-oxy-fucoxanthin, 19-Hex) in 6 seawater enclosures which were perturbed by bubbling with ambient air (400 ppmv CO₂, Low CO₂ level) or an air/CO₂ mixture at a concentration of 1000 ppmv CO₂ (High CO₂ level). Symbols are the means and error bars are the standard errors of three replicate enclosures.

degradation¹⁷. In coastal eutrophic seawater, the concentration of labile DOC is high. In our system, the initial concentration was more than 200 µM. It is obvious that the decomposition of DOC led to the high *p*CO₂ in the initial water (805 µatm). Although the initial *p*CO₂ in the water in our study was much higher than the atmospheric CO₂, the continued aeration in HC enclosures further exacerbated the pre-existing ocean acidification and reduced the pH (800–1000 ppm, Figs 1 and 2). The continued aeration of 400 ppm air reflects the initially high *p*CO₂ water gradually returning to the air sea equilibrium state (400–800 ppm) by the exchange with ambient *p*CO₂ air. Our results confirm the two states. The mean *p*CO₂ levels in the HC and LC treatments were 879.15 ± 145.76 and 658.05 ± 113.98 ppmv, with the significant differences of 221.10 ppmv in the first 4 days (Fig. 2b). Therefore, the results of this study may inform us about phytoplankton responses during a similar natural bloom in current low-pH coastal eutrophic environments under higher atmospheric CO₂ concentrations in the future.

Many previous mesocosm studies were conducted in high latitude waters (Table S1), where low temperatures lead to high solubility of CO₂, and potentially larger biological effects of acidification^{6,7}. Our work is the first mesocosm CO₂ perturbation study in a eutrophic subtropical ecosystem (24.5°N, 118.2°E) and thus could

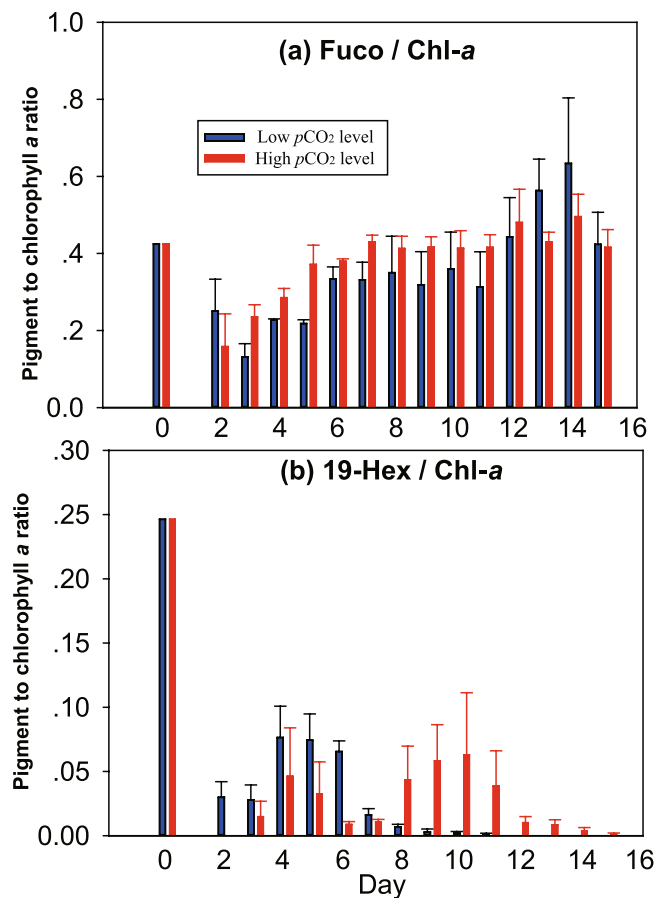


Figure 7. Temporal variations in ratios of fucoxanthin (**a**, Fuco) and 19^hhexanoyl-oxy-fucoxanthin (**b**, Hex-Fuco) to chlorophyll *a* in 6 seawater enclosures which were perturbed by bubbling with ambient air (400 ppmv CO₂, Low CO₂ level) or an air/CO₂ mixture at a concentration of 1000 ppmv CO₂ (High CO₂ level). Columns are the means and error bars are the standard errors of three replicate enclosures.

	Enclosures	Net calcification rate (μmol·kg ⁻¹ ·d ⁻¹)	POC production rate (μmol·L ⁻¹ ·d ⁻¹)	DOC production rate (μmol·L ⁻¹ ·d ⁻¹)	PIC:POC ratio
HC	1	1.22	12.60	32.30	0.10
	3	1.22	— ^a	31.90	—
	5	1.36	27.80	24.80	0.05
	Mean	1.27	20.20	29.67	0.08
	SD	0.08	10.75	4.22	0.04
LC	2	1.44	3.72	21.00	0.39
	4	1.64	9.15	10.90	0.18
	6	1.65	13.60	10.60	0.12
	Mean	1.58	8.82	14.17	0.23
	SD	0.12	4.95	5.92	0.14

Table 1. The overall particulate inorganic carbon (PIC), particulate organic carbon (POC) and dissolved organic carbon (DOC) production rates and PIC:POC ratios during the mesocosm incubations for 15 days under present and elevated partial pressure of CO₂ ($p\text{CO}_2 = 400$ and 1000 ppmv, respectively) in triplicate 4 m³ enclosures. ^aPOC samples were not collected in this enclosure during the experiment.

be comparable to the previous mesocosm experiment in the coastal waters of Korea (34.6°N and 128.5°E)^{14,18}. However, the Korean experiments were performed in winter. More importantly, these previous studies were done by adding inorganic nutrients to trigger algae blooms. While, we used natural sea water after filtering out particles (< 0.01 μm). The high nutrient concentration is its own characteristics (eutrophication in Chinese coastal water). Nutrients concentrations, nutrients compositions (N/P/Si, NH₄⁺/NO_x, DIN/DON) and other factors (such as metals) were the same as the *in-situ* seawater with a salinity of 27.3.

In the HC treatment, clear enhancement of phytoplankton total Chl-*a* biomass and diagnostic pigment concentrations of both diatom and prymnesiophytes were observed (Fig. 6). These results are consistent with the production of particulate and dissolved organic carbon in the HC enclosures (Table 1). The increases in pH and DIN/DIC/ $p\text{CO}_2$ drawdown due to phytoplankton growth during the experiment were also larger in the HC scenario than those of the LC treatment (Figs 1–3). Similar to our results, increasing inorganic carbon concentrations have been shown to enhance primary production¹⁹ and carbon assimilation in various photoautotrophs. Of course, studies have reported similar results for diatoms²⁰ and coccolithophores²¹ in mono-culture. Growth of a natural phytoplankton community was also stimulated by elevated CO_2 in an Arctic mesocosm experiment, leading to enhanced nutrient uptake and higher biomass build-up right after dissolved inorganic nutrient addition¹⁶. The enhanced production and exudation of organic matter in particular stimulated microbial loop activities and altered food web structure⁷.

It has been suggested that CO_2 could limit carbon fixation by marine phytoplankton and by large diatoms in particular, as the free CO_2 concentration is usually below that required for half saturation of Ribulose-1, 5-bisphosphate Carboxylase Oxygenase (RUBISCO), the core carbon-fixing enzyme in photosynthesis. There is experimental support for this idea^{20,22}, even though most phytoplankton can utilize cellular C-concentrating mechanisms (CCM) based on the active uptake of CO_2 and/or HCO_3^- from the environment²³. The quite high pH values (8.90) and low $p\text{CO}_2$ in water (31 μatm) on day 10 in our HC treatments also indicate that there might be insufficient CO_2 for phytoplankton (Figs 1 and 2). For diatoms (*Phaeodactylum tricornutum*), previous studies showed that growth and photosynthetic carbon fixation rates were enhanced by the enrichment of CO_2 under low or moderate levels of light²⁴, though photosynthetic inorganic carbon affinity was down regulated by 20% under the high CO_2 condition²². Therefore, it is reasonable to infer that the growth of phytoplankton in eutrophic water, in particular that of large diatoms²⁵, can be enhanced by high CO_2 (Fig. 6 and Table 1).

However, there are also reports of neutral responses and even negative effects²⁶. Species-specific CO_2 responses could result from taxonomic differences among phytoplankton in the physiological mechanisms of CO_2 uptake²⁷. In addition to increased $p\text{CO}_2$ in seawater under HC, lowered pH can lead to acidic stress. The lower calcification rates (Table 1) reflect a more rapid dissolution of CaCO_3 or reduced rates of calcification in the low pH enclosures²⁸. The difference on the ratios of PIC:POC between treatments suggest two opposing effects on the production of organic and inorganic carbon, respectively (Table 1). The lowered pH may also reduce the ability of some species to tolerate high light stress, resulting in increases in respiratory carbon loss²⁹. Thus, whether or not phytoplankton will benefit from increased CO_2 remains controversial²⁶, since species-specific behavior and different physiological processes in different waters or experimental conditions are involved^{29,30}. In eutrophic coastal waters where diatoms dominated in the phytoplankton community, our results support the general proposition that increasing CO_2 may promote phytoplankton photosynthesis and growth^{7,15}.

Species composition under high CO_2 . Changes in dissolved aqueous CO_2 may affect phytoplankton community structure³¹. A meta-analysis of published experimental data emphasized that the differing responses to elevated $p\text{CO}_2$ caused sufficient changes between phytoplankton types in competitive fitness to significantly alter community structure³². Our results indicate a rapid response of prymnesiophytes in the HC treatment, while a short time-lag was observed in the stimulation of diatom growth (Figs 6 and 7). This response was the opposite of the expected trend, by which large phytoplankton should grow faster than small phytoplankton in nutrient replete conditions while the latter have the advantage in oligotrophic environments. This unexpected result could be due to the greater contribution of NH_4^+ to total DIN compared to NO_3^- , as prymnesiophytes began to decline in day 6 when NH_4^+ was depleted (Figs 3 and 6). Results of an Arctic mesocosm experiment also indicated a positive effect of HC on pico- and nano-eukaryotes during the nutrient replete phase¹⁶. The authors of this study suggested that if cells are small enough that their dissolved inorganic carbon supply needs can be met at least partly by diffusion, higher seawater CO_2 concentrations could stimulate photosynthetic carbon fixation and growth in these species¹⁶.

Our study indicates that diatoms have an overall advantage in eutrophic HC waters compared to prymnesiophytes, although the initial Chl-*a* concentrations of both groups were the same and the initial cell numbers of prymnesiophytes were even higher than those of diatoms (Fig. 6). As mentioned above, the decreased affinity for HCO_3^- or/and CO_2 and down-regulated CCM in diatom can save CCM-operational energy^{22,33}, so that increased CO_2 availability can be beneficial in terms of energetics. In contrast, prymnesiophytes could have a competitive advantage over diatoms in low CO_2 environments³⁴. Similarly, it was observed a clear succession from prymnesiophytes to diatoms when CO_2 concentrations increased from 150 to 750 ppmv³¹. Another experimental study in the North Atlantic Ocean, however, showed a shift away from diatoms and towards coccolithophores under HC, warmer conditions³⁵. It has been suggested that paleoceanographic data showing lower Si:N utilization ratios by phytoplankton during the last glacial maximum could be due to community shifts towards non-siliceous species such as prymnesiophytes caused by decreased CO_2 in the glacial atmosphere (180 ppmv)³¹, although other studies have attributed lower Si:N utilization ratios and export of biogenic Si to relaxed iron limitation of diatoms during glacial periods³⁶. In addition, other factors are likely to be also important, such as light. Prymnesiophytes can grow fast and make dense blooms, but they also like high light conditions³⁷. In a mesocosm where Chl-*a* reaches such high concentrations, light must be much reduced through self-shading, possibly not favoring prymnesiophyte growth.

Effects on stoichiometry. Overconsumption of carbon relative to nutrient uptake has been reported in several studies of the planktonic response to increased CO_2 ^{9,20,38}. For the same uptake of inorganic nutrients, net community carbon consumption under increased CO_2 exceeded present rate by 27 and 39% in 700 and 1050 μatm respectively¹. However, many other studies have found contrary trends or no effect of high CO_2 on C:N ratios^{10,13,14,18,39}. Differing effects of HC on stoichiometric uptake ratios (Table S1) may be attributed to

the different biogeochemical demands of the dominant plankton functional types, and life stage-specific biogeochemical requirements¹³.

Our results indicate a clear increase in N:P and N:Si consumption ratios under HC treatments throughout the experiment, supporting higher Chl-*a* and production (Figs 3–6 and Table 1). In other words, assimilations of SRP and SiO₃²⁻ may be reduced relative to that of nitrogen in eutrophic coastal environments under high CO₂. A previous study reported that C:P, in contrast to the C:N response, increased significantly in the post-bloom phase¹⁸. An Arctic mesocosm project with higher CO₂ had higher POC/POP and PON/POP during the nutrient rich phase¹⁶. Based on our results, the differences in N:P and N:Si consumption ratios between the two treatments (Figs 4 and 5) were completely due to changes in nitrate drawdown (Fig. 3C). Previous study revealed that elevated *p*CO₂ strikingly reduced NO₃⁻ uptake and assimilation in the diatom *Thalassiosira pseudonana* at both high and low light, as indicated by both short-term and steady-state net NO₃⁻ uptake rates, which was further supported by the reduced gene transcription, protein expression and enzymatic activity of nitrate reductase at high CO₂³³. In parallel, diminished NO₃⁻ uptake at elevated *p*CO₂ resulted in lower PON and total protein content⁴⁰. This could be more important for larger diatoms as they require a greater fraction (by 3.5-fold compared with small ones) of their total cellular nitrogen to RUBISCO for maintaining carbon fixation, hence a higher nitrogen cost in larger diatoms for RUBISCO leads to higher nitrogen requirements²⁵. In addition, accumulating evidence suggests that the nitrogen cycle may respond strongly to higher *p*CO₂ through increases in global N₂ fixation⁴¹ and possibly denitrification⁴², as well as decreases in nitrification⁴³.

In contrast, to date, most studies have found negligible or minor effects of projected future changes in *p*CO₂ on most phytoplankton phosphorus requirements¹⁰. If indeed N:P and N:Si consumption ratios are elevated under HC environment, the P and Si limitation often observed in fresh and coastal waters will be possibly eased by lower consumption of SRP and Si under HC conditions, relative to the same uptake of DIN (Figs 3 and 4). This is also likely to be the cause of higher Chl-*a* biomass in HC environments with the same initial nutrient concentrations (Fig. 6).

Moreover, the ongoing increase in wind-driven upwelling⁴⁴ and anthropogenic nutrient inputs in coastal systems⁴⁵ may increase nutrient inputs and blooms in coastal waters⁴⁶. The sustained increase in nitrate loading from the Mississippi River⁴⁷, the Pearl River⁴⁸ and the Changjiang River⁴⁹ has resulted in rapidly rising nutrient ratios (N:P and N:Si) since the 1950s, due to increased use of agricultural fertilizers. Associated with the higher Chl-*a* biomass, species succession and eased P and/or Si limitation discussed above, our study further suggests that future climate and land use changes may result in even more serious and complicated interactive effects of eutrophication, ocean acidification and hypoxia in coastal waters^{3,50}.

Conclusions

Shallow coastal areas are vulnerable to the effects of human development, and can receive massive loads of fresh water, nutrients, and organic and inorganic carbon. In this study, a mesocosm CO₂ perturbation study was conducted to investigate the effect of rising CO₂ on a model plankton community in a eutrophic subtropical bay in China. Although the initial DIC and further decomposition of organic matter led to the *p*CO₂ in the coastal water being much higher than that in the air, further enrichment of CO₂ appeared to be conducive to the production and biomass of both diatoms and prymnesiophytes. Diatoms had a clear advantage in this highly eutrophic water under the elevated CO₂ concentration. However, prymnesiophytes seemingly responded rapidly in the HC enclosures, whereas a time lag was observed in diatom growth. Compared with the low CO₂ treatments, the N/P and N/Si consumption ratios significantly increased during the growth of phytoplankton at higher CO₂ partial pressure. These results indicate complex effects induced by ocean acidification in phytoplankton stoichiometry, production and community structure in eutrophic coastal waters which may have serious consequences for these biologically and economically important ecosystems.

Material and Methods

Experimental setup and sampling. The Xiamen University mesocosm facility for ocean acidification impacts study (FOANIC-XMU, <http://mel.xmu.edu.cn/dynamicfile.asp?id=76>) was deployed in Wuyuan Bay, Xiamen, China (24.5°N, 118.2°E)⁵¹. The dimensions of the floating platform are 28 × 10 m, and the facility includes 9 mesocosm enclosures immersed in the seawater along the south side of the platform to avoid shading (Supplementary Material, Fig. S1). The enclosures are 3 m deep and 1.5 m wide, with 50 cm projecting above the sea surface. The volume of the enclosures was 4 m³, and they were composed of a 0.9 mm thick cylindrical transparent thermoplastic polyurethane plastic membrane that is partially transparent to UV. The mesocosms are covered with plastic domes to reduce the contamination risk and prevent rainfall from diluting the experiments.

In order to minimize the influences of other groups of organisms such as grazers, and remove non-living suspended particles that would potentially affect the later measurements of biogenic elements, *in situ* seawater was filtered through a water purifier (MU801-4T, Midea) which was equipped with 0.01 μm pore size cartridges, and simultaneously injected into the enclosures. Then 0.2 g L⁻¹ of NaCl solution was added into each mesocosm to determine the exact volume by comparison of the salinity before and after salt addition. Ocean acidification conditions were induced gradually with aeration using CO₂ enrichers (CE-100, Wuhan Ruihua Instrument & Equipment, China). The *p*CO₂ of seawater in 6 of the enclosures was perturbed by bubbling with free air (ambient CO₂, ~400 ppmv, denoted LC) or using an air/CO₂ mixture at the concentration of 1000 ppmv (denoted HC). The air with different CO₂ concentrations was delivered into the seawater at a flow rate of ~5 L min⁻¹ with 6 mm diameter plastic tubing, and dispersed by an air stone disk placed in the center of each mesocosm's bottom. The bubbling was continued for the duration of the whole experiment.

The species interactions of natural populations are typically extremely complicated, depending on the abundance and intrinsic properties of various species as well as other abiotic and biotic factors. Therefore, four well-studied phytoplankton species were used in this study, including the diatoms *Phaeodactylum tricornutum*

(CCMA 106, from Center for Collections of Marine Algae, Xiamen University) and *Thalassiosira weissflogii* (CCMP 102, from The National Center for Marine Algae and Microbiota, USA), and the coccolithophores *Emiliania huxleyi* (CS-369, from Commonwealth Scientific and Industrial Research Organization, Australia) and *Gephyrocapsa oceanica* (NIES-1318, National Institute for Environmental Studies, Japan), were first mono-cultured indoors at 400 and 1000 ppmv CO₂. They were acclimated for 10 days (about 10–15 generations) at 20 °C and 150 μmol m⁻² s⁻¹ (cool white fluorescence) irradiance using the same eutrophic bay seawater later used for the experiments, collected and filtered *in situ* without nutrient additions. After the acclimation period, these species were inoculated into each enclosure with equivalent chlorophyll *a* (Chl-*a*), respectively, at a total final abundance of 5.07 × 10⁴ cells L⁻¹. The initial abundances of *Phaeodactylum tricoratum*, *Thalassiosira weissflogii*, *Emiliania huxleyi* and *Gephyrocapsa oceanica* were about 10000, 700, 20000 and 20000 cells L⁻¹, respectively. The initial cell concentrations were set up based on their differences in size and Chl-*a* per cell to yield similar initial biomass levels. The growth of these phytoplankton groups was studied for 15 days (15 to 30 June, 2013) under present and elevated partial pressure of CO₂ (pCO₂ = 400 and 1000 ppmv, respectively) in triplicate 4 m³ enclosures.

Environmental factors. The salinity, temperature and pH profiles in the mesocosm were measured daily at 10:00 AM with a CTD (RBR) or a SeaFET (Satalantic). Due to aeration, these profiles indicated the water in each enclosure was homogenized (Supplementary Material, Fig. S2). The subsamples for chemical and biological determinations were taken at the middle of the mesocosms with a water sampler. The total amount of water for sampling from the enclosures was less than 5% of the initial volume. The pH values were determined using the pH indicator meta-cresol purple with a spectrophotometer (Agilent 8453), with a measurement accuracy of ± 0.0005. The CO₂ partial pressure in the seawater (pCO₂) was calculated by the program CO2SYS⁵² from dissolved inorganic carbon (DIC) and total alkalinity (TA)^{53,54}.

Nutrient samples for NO₃⁻ + NO₂⁻ (NO_x), NH₄⁺ and soluble reactive phosphate (SRP) were filtered immediately after collection through 47 mm GF/F filters and were then frozen at -20 °C. Samples for SiO₃²⁻ were filtered through acid-cleaned 0.45 μm pore size acetate cellulose filters and were kept refrigerated at 4 °C. Filtrates for NH₄⁺ and SiO₃²⁻ were preserved with 100 μL CCl₄. All the nutrient samples were measured in our land-based laboratory at Xiamen University within 15 days after the mesocosm experiment. Nutrient samples for NO_x, SRP and SiO₃²⁻ were analysed using a four-channel continuous-flow Technicon AA3 Auto-Analyzer (Bran-Lube GmbH)⁵⁵. NO_x was analyzed using the copper-cadmium column reduction method⁵. SRP and SiO₃²⁻ were measured using typical spectrophotometric methods⁵⁶. NH₄⁺ was run with a 722 type spectrophotometer (Xiamen Analytical Instrument Co., China) according to the indophenol blue spectrophotometric method^{5,57}. The precision for nutrient analyses in this study was ≤ 3%, and the detection limits for NO_x, SRP, SiO₃²⁻ and NH₄⁺ analyses were 0.03, 0.03, 0.05 and 0.16 μM, respectively.

Phytoplankton biomass and community structure. Photosynthetic pigment concentrations were measured by high-performance liquid chromatography (HPLC) using a Shimadzu 20 A HPLC system fitted with a 3.5 μm Eclipse XDB C₈ column (4.6 × 150 mm, Agilent Technologies, Waldbronn, Germany), as in our previous studies^{8,58}. Briefly, seawater samples for phytoplankton pigment analysis (0.2–2 L, according to biomass) were filtered through 25 mm GF/F glass fiber filters (under a vacuum pressure < 10 kPa under dim light), and then they were immediately frozen (-80 °C) until analysis in the laboratory within 30 days. Phytoplankton pigments were extracted in N, N-dimethylformamide and analyzed. The concentrations of chlorophyll *a* (Chl-*a*), diagnostic pigments of diatoms, (fucoxanthin, Fuco) and prymnesiophytes (19'-hexanoyl-oxy-fucoxanthin, 19-Hex) were detected, and quantified using standards that were purchased from DHI Water & Environment, Hørsholm, Denmark.

Pigment samples of the four phytoplankton species were collected in exponential growth phase during mono-culture under indoor conditions to obtain the ratios of diagnostic pigments to Chl-*a* for CHEMTAX analyses^{8,58}. These initial pigments ratios might be quite different from those of the same species grown under sunlight in the mesocosms. To confirm the phytoplankton community structure based on pigments information, a 0.5 L water sample was collected and preserved with Lugol's iodine solution for microscopic observation. The Chl-*a* concentrations were also compared to the cell number, and these two values were significantly correlated (Supplementary Material, Fig. S3, R² = 0.76, n = 27, p < 0.01).

Carbon metabolism. Net calcification rate was estimated by the TA anomaly method⁵⁹. TA was measured by potentiometric titration using the Gran procedure⁶⁰. In addition, TA has to be corrected for the effect of primary production, i.e., since an uptake of 1 mol NO₃⁻ or PO₄³⁻ increases TA by 1 mole⁵⁹, and an uptake of 1 mol NH₄⁺ decreases TA by 1 mole⁶¹. Thus, the net calcification rate can be estimated as equation (1).

$$\text{Net calcification rate} = -0.5 \times (\Delta TA_{\text{measured}} - \Delta \text{NO}_3^- - \Delta \text{PO}_4^{3-} + \Delta \text{NH}_4^+) / \Delta t \quad (1)$$

For particulate organic carbon (POC) sampling, seawater was filtered through a pre-combusted 47 mm GF/F filter (Whatman). Prior to analysis, the filters were frozen at -20 °C and POC (via acid fuming) was determined with a PE-2400 SERIES IICHNS/O analyzer according to the JGOFS protocols⁵⁶. Dissolved organic carbon (DOC) samples were filtering onto pre-combusted 25 mm GF/F filters and stored in pre-combusted EPA vials at -20 °C until analysis using a Shimadzu TOC-V Analyzer⁶². The overall POC and DOC production rates for 15 days (day 0–day 14) were calculated according to the following equations:

$$\text{POC production rate} = \Delta \text{POC} / \Delta t \quad (2)$$

$$\text{DOC production rate} = \Delta\text{DOC}/\Delta t \quad (3)$$

Since particulate inorganic carbon (PIC) samples were limited, we assumed that all PIC is in the form of CaCO_3 . Accordingly, the PIC value in this study was calculated with the following formula⁶³:

$$\Delta\text{PIC}_{\text{calculated}} = \text{CaCO}_3 \text{ accumulation} = -0.5 \times (\Delta\text{TA}_{\text{measured}} - \Delta\text{NO}_3^- - \Delta\text{PO}_4^{3-} + \Delta\text{NH}_4^+) \quad (4)$$

In all the formulas above, ΔTA , ΔNO_3^- , ΔPO_4^{3-} , ΔNH_4^+ , ΔDOC , ΔPOC , $\Delta\text{PIC}_{\text{calculated}}$ denote the changes of these parameters, and Δt denotes the elapsed time. A one-way ANOVA was used for statistical analysis following a test for homogeneity of the variances. The significance level was set at $p < 0.05$. ANOVA results were compared using the Tukey HSD method.

References

- Riebesell, U. *et al.* Enhanced biological carbon consumption in a high CO_2 ocean. *Nature* **450**, 545–548, doi:10.1038/nature06267 (2007).
- Busch, D. S. *et al.* Understanding, characterizing, and communicating responses to ocean acidification: challenges and uncertainties. *Oceanography* **25**, 30–39, doi:10.5670/oceanog.2015.29 (2015).
- Cai, W. J. *et al.* Acidification of subsurface coastal waters enhanced by eutrophication. *Nat. Geosci.* **4**, 766–770, doi:10.1038/Ngeo1297 (2011).
- Zhai, W., Dai, M., Cai, W. J., Wang, Y. & Wang, Z. High partial pressure of CO_2 and its maintaining mechanism in a subtropical estuary: the Pearl River estuary, China. *Mar. Chem.* **93**, 21–32, doi:10.1016/j.marchem.2004.07.003 (2005).
- Dai, M. *et al.* Nitrification and inorganic nitrogen distribution in a large perturbed river/estuarine system: the Pearl River estuary, China. *Biogeosciences* **5**, 1227–1244 (2008).
- Riebesell, U., Bellerby, R. G. J., Grossart, H. P. & Thingstad, F. Mesocosm CO_2 perturbation studies: from organism to community level. *Biogeosciences* **5**, 1157–1164, doi:10.5194/bg-5-1157-2008 (2008).
- Riebesell, U., Gattuso, J. P., Thingstad, T. F. & Middelburg, J. J. “Arctic ocean acidification: pelagic ecosystem and biogeochemical responses during a mesocosm study”. *Biogeosciences* **10**, 5619–5626, doi:10.5194/bg-10-5619-2013 (2013).
- Liu, X. *et al.* Responses of phytoplankton communities to environmental variability in the East China Sea. *Ecosystems* **19**, 832–849, doi:10.1007/s10021-016-9970-5 (2016).
- Bellerby, R. G. J. *et al.* Marine ecosystem community carbon and nutrient uptake stoichiometry under varying ocean acidification during the PeECE III experiment. *Biogeosciences* **5**, 1517–1527, doi:10.5194/bg-5-1517-2008 (2008).
- Hutchins, D. A., Mulholland, M. R. & Fu, F. Nutrient Cycles and Marine Microbes in a CO_2 -Enriched Ocean. *Oceanography* **22**, 128–145, doi:10.5670/oceanog.2009.103 (2009).
- Riebesell, U. & Gattuso, J. P. Lessons learned from ocean acidification research. *Nat. Clim. Change.* **5**, 12–14 (2015).
- Tatters, A. O. *et al.* Short- and long-term conditioning of a temperate marine diatom community to acidification and warming. *Philos. Trans. R. Soc. Lond. B. Biol. Sci.* **368**, 20120437, doi:10.1098/rstb.2012.0437 (2013).
- Silyakova, A. *et al.* Pelagic community production and carbon-nutrient stoichiometry under variable ocean acidification in an Arctic fjord. *Biogeosciences* **10**, 4847–4859, doi:10.5194/bg-10-4847-2013 (2013).
- Kim, J. M. *et al.* Shifts in biogenic carbon flow from particulate to dissolved forms under high carbon dioxide and warm ocean conditions. *Geophys. Res. Lett.* **38**, L08612, doi:10.1029/2011gl047346 (2011).
- Kim, J. H. *et al.* Enhancement of photosynthetic carbon assimilation efficiency by phytoplankton in the future coastal ocean. *Biogeosciences* **10**, 7525–7535, doi:10.5194/bg-10-7525-2013 (2013).
- Schulz, K. G. *et al.* Temporal biomass dynamics of an Arctic plankton bloom in response to increasing levels of atmospheric carbon dioxide. *Biogeosciences* **10**, 161–180, doi:10.5194/bg-10-161-2013 (2013).
- Wu, K. *et al.* Dissolved organic carbon in the South China Sea and its exchange with the Western Pacific Ocean. *Deep Sea Res. II* **122**, 41–51, doi:10.1016/j.dsr2.2015.06.013 (2015).
- Kim, J. M. *et al.* The effect of seawater CO_2 concentration on growth of a natural phytoplankton assemblage in a controlled mesocosm experiment. *Limnol. Oceanogr.* **51**, 1629–1636 (2006).
- Hein, M. & Sand-Jensen, K. CO_2 increases oceanic primary production. *Nature* **388**, 526–527, doi:10.1038/41457 (1997).
- Riebesell, U., Wolf-Gladrow, D. A. & Smetacek, V. Carbon dioxide limitation of marine phytoplankton growth rates. *Nature* **361**, 249–251 (1993).
- Feng, Y. *et al.* Interactive effects of increased $p\text{CO}_2$, temperature and irradiance on the marine coccolithophore *Emiliania huxleyi* (Prymnesiophyceae). *Eur. J. Phycol.* **43**, 87–98 (2008).
- Wu, Y., Gao, K. & Riebesell, U. CO_2 -induced seawater acidification affects physiological performance of the marine diatom *Phaeodactylum tricoratum*. *Biogeosciences* **7**, 2915–2923, doi:10.5194/bg-7-2915-2010 (2010).
- Raven, J. A., Giordano, M., Beardall, J. & Maberly, S. C. Algal and aquatic plant carbon concentrating mechanisms in relation to environmental change. *Photosynthesis Res.* **109**, 281–296, doi:10.1007/s11120-011-9632-6 (2011).
- Gao, K. S. & Campbell, D. A. Photophysiological responses of marine diatoms to elevated CO_2 and decreased pH: a review. *Funct. Plant Biol.* **41**, 449–459, doi:10.1071/FP13247 (2014).
- Wu, Y., Jeans, J., Suggett, D. J., Finkel, Z. V. & Campbell, D. A. Large centric diatoms allocate more cellular nitrogen to photosynthesis to counter slower RUBISCO turnover rates. *Front. Mar. Sci.* **1**, 1–11, doi:10.3389/fmars.2014.00068 (2014).
- Mackey, K., Morris, J. J., Morel, F. & Kranz, S. Response of photosynthesis to ocean acidification. *Oceanography* **25**, 74–91, doi:10.5670/oceanog.2015.33 (2015).
- Raven, J. A. & Johnston, A. M. Mechanisms of inorganic-carbon acquisition in marine phytoplankton and their implications for the use of other resources. *Limnol. Oceanogr.* **36**, 1701–1714 (1991).
- Riebesell, U. *et al.* Reduced calcification of marine plankton in response to increased atmospheric CO_2 . *Nature* **407**, 364–367 (2000).
- Gao, K., Helbling, E. W., Häder, D. P. & Hutchins, D. A. Responses of marine primary producers to interactions between ocean acidification, solar radiation, and warming. *Mar. Ecol. Prog. Ser.* **470**, 167–189, doi:10.3354/meps10043 (2012).
- Wu, H. Y., Zou, D. H. & Gao, K. S. Impacts of increased atmospheric CO_2 concentration on photosynthesis and growth of micro- and macro-algae. *Sci. China Ser. C* **51**, 1144–1150, doi:10.1007/s11427-008-0142-5 (2008).
- Tortell, P. D., DiTullio, G. R., Sigman, D. M. & Morel, F. M. M. CO_2 effects on taxonomic composition and nutrient utilization in an equatorial Pacific phytoplankton assemblage. *Mar. Ecol. Prog. Ser.* **236**, 37–43, doi:10.3354/Meps236037 (2002).
- Dutkiewicz, S. *et al.* Impact of ocean acidification on the structure of future phytoplankton communities. *Nat. Clim. Change.* **5**, 1002–1006, doi:10.1038/nclimate2722 (2015).
- Shi, D. *et al.* Interactive effects of light, nitrogen source, and carbon dioxide on energy metabolism in the diatom *Thalassiosira pseudonana*. *Limnol. Oceanogr.* **60**, 1805–1822, doi:10.1002/lno.10134 (2015).
- Hinga, K. R. Co-occurrence of dinoflagellate blooms and high pH in marine enclosures. *Mar. Ecol. Prog. Ser.* **86**, 181–181 (1992).
- Feng, Y. *et al.* Effects of increased $p\text{CO}_2$ and temperature on the North Atlantic spring bloom. I. The phytoplankton community and biogeochemical response. *Mar. Ecol. Prog. Ser.* **388**, 13–25, doi:10.3354/meps08133 (2009).

36. Hutchins, D. A. & Bruland, K. W. Iron-limited diatom growth and Si: N uptake ratios in a coastal upwelling regime. *Nature* **393**, 561–564 (1998).
37. Ziveri, P., Broerse, A. T. C., van Hinte, J. E., Westbroek, P. & Honjo, S. The fate of coccoliths at 48°N 21°W, northeastern Atlantic. *Deep Sea Res. II* **47**, 1853–1875 (2000).
38. Zark, M., Riebesell, U. & Dittmar, T. Effects of ocean acidification on marine dissolved organic matter are not detectable over the succession of phytoplankton blooms. *Science Advances* **1**, e1500531, doi:10.1126/sciadv.1500531 (2015).
39. Engel, A. *et al.* Testing the direct effect of CO₂ concentration on a bloom of the coccolithophorid *Emiliania huxleyi* in mesocosm experiments. *Limnol. Oceanogr.* **50**, 493–507, doi:10.4319/lo.2005.50.2.0493 (2005).
40. Hennon, G. M. M., Quay, P., Morales, R. L., Swanson, L. M. & Armbrust, E. V. Acclimation conditions modify physiological response of the diatom *Thalassiosira pseudonana* to elevated CO₂ concentrations in a nitrate-limited chemostat. *J. Phycol.* **50**, 243–253, doi:10.1111/jpy.12156 (2014).
41. Hutchins, D. *et al.* CO₂ control of *Trichodesmium* N₂ fixation, photosynthesis, growth rates, and elemental ratios: Implications for past, present, and future ocean biogeochemistry. *Limnol. Oceanogr.* **52**, 1293 (2007).
42. Fennel, K., Wilkin, J., Previdi, M. & Najjar, R. Denitrification effects on air-sea CO₂ flux in the coastal ocean: Simulations for the northwest North Atlantic. *Geophys. Res. Lett.* **35** (2008).
43. Beman, J. M. *et al.* Global declines in oceanic nitrification rates as a consequence of ocean acidification. *Proc. Natl. Acad. Sci. USA* **108**, 208–213, doi:10.1073/pnas.1011053108 (2011).
44. Bakun, A. Global climate change and intensification of coastal ocean upwelling. *Science* **247**, 198–201, doi:10.1126/science.247.4939.198 (1990).
45. Kim, I. N. *et al.* Increasing anthropogenic nitrogen in the North Pacific. *Ocean. Science* **346**, 1102–1106, doi:10.1126/science.1258396 (2014).
46. Glibert, P. M. *et al.* Vulnerability of coastal ecosystems to changes in harmful algal bloom distribution in response to climate change: projections based on model analysis. *Global. Change. Biol.* **20**, 3845–3858, doi:10.1111/gcb.12662 (2014).
47. Rabalais, N. N. *et al.* Hypoxia in the northern Gulf of Mexico: Does the science support the plan to reduce, mitigate, and control hypoxia? *Estuar. Coast.* **30**, 753–772 (2007).
48. Harrison, P., Yin, K., Lee, J., Gan, J. & Liu, H. Physical–biological coupling in the Pearl River estuary. *Cont. Shelf. Res.* **28**, 1405–1415, doi:10.1016/j.csr.2007.02.011 (2008).
49. Zhou, M. J., Shen, Z. L. & Yu, R. C. Responses of a coastal phytoplankton community to increased nutrient input from the Changjiang (Yangtze) River. *Cont. Shelf. Res.* **28**, 1483–1489, doi:10.1016/j.csr.2007.02.009 (2008).
50. Greene, R. M., Lehrter, J. C. & Hagy, J. D. Multiple regression models for hindcasting and forecasting midsummer hypoxia in the Gulf of Mexico. *Ecol. Appl.* **19**, 1161–1175 (2009).
51. Xing, T., Wu, Y. P., Ding, J. C. & Gao, K. S. Diurnal light utilization efficiency of phytoplankton is decreased by elevated CO₂ concentration: a mesocosm experiment. *Fundam. Appl. Limnol.* **188**, 83–92 (2016).
52. Lewis, E., Wallace, D. & Allison, L. J. *Program developed for CO₂ system calculations*. (Carbon Dioxide Information Analysis Center, managed by Lockheed Martin Energy Research Corporation for the US Department of Energy Tennessee, 1998).
53. Langdon, C. & Atkinson, M. J. Effect of elevated pCO₂ on photosynthesis and calcification of corals and interactions with seasonal change in temperature/irradiance and nutrient enrichment. *J. Geophys. Res. (Oceans)* **110**, doi:10.1029/2004jc002576 (2005).
54. Millero, F. J. In *Chemical Oceanography* (ed Frank J Millero) 259–329 (CRC press, 2013).
55. Han, A. *et al.* Nutrient dynamics and biological consumption in a large continental shelf system under the influence of both a river plume and coastal upwelling. *Limnol. Oceanogr.* **57**, 486–502, doi:10.4319/lo.2012.57.2.0486 (2012).
56. Knap, A. H., Michaels, A., Close, A. R., Ducklow, H. & Dickson, A. G. Protocols for the joint global ocean flux study (JGOFS) core measurements. *JGOFS, Reprint of the IOC Manuals and Guides No. 29, UNESCO 1994* **19** (1996).
57. Pai, S. C., Tsau, Y. J. & Yang, T. I. pH and buffering capacity problems involved in the determination of ammonia in saline water using the indophenol blue spectrophotometric method. *Anal. Chim. Acta* **434**, 209–216 (2001).
58. Liu, X. *et al.* High-resolution phytoplankton diel variations in the summer stratified central Yellow Sea. *J. Oceanogr.* **68**, 913–927, doi:10.1007/s10872-012-0144-6 (2012).
59. Delille, B. *et al.* Response of primary production and calcification to changes of pCO₂ during experimental blooms of the coccolithophorid *Emiliania huxleyi*. *Global Biogeochem. Cycles* **19**, GB2023, doi:10.1029/2004gb002318 (2005).
60. Wang, Z. A. & Cai, W. J. Carbon dioxide degassing and inorganic carbon export from a marsh-dominated estuary (the Duplin River): A marsh CO₂ pump. *Limnol. Oceanogr.* **49**, 341–354 (2004).
61. Wolf-Gladrow, D. A., Zeebe, R. E., Klaas, C., Körtzinger, A. & Dickson, A. G. Total alkalinity: The explicit conservative expression and its application to biogeochemical processes. *Mar. Chem.* **106**, 287–300 (2007).
62. Dai, M. *et al.* Excess total organic carbon in the intermediate water of the South China Sea and its export to the North Pacific. *Geochem Geophys Geosy* **10**, Q12002, doi:10.1029/2009gc002752 (2009).
63. De Bodt, C., Harlay, J. & Chou, L. Biocalcification by *Emiliania huxleyi* in batch culture experiments. *Mineral. Mag.* **72**, 251–256 (2008).

Acknowledgements

This work was supported by grants from the National Key R&D Program of China (No. 2016YFA0601203), and the China NSF (Nos. 41406143, 41430967, 41120164007, 41330961, and 41206091), State Oceanic Administration (National Program on Global Change and Air-Sea Interaction, GASI-03-01-02-04), and the U.S. National Science Foundation Biological Oceanography (OCE 1538525). Visit of DH and FF was supported by “111” project. We would like to thank Tao Huang and Shuimiao Lu for help with the data collection. We also thank Yahe Li, Nana Liu, Liguang Guo, Jianzhong Su, Zhoulun Zhang, Peng Jin, Wei Li, Jiancheng Ding, Futian Li, Tifeng Wang, Shanying Tong, Tao Xing, Jie Zhou, and Juntian Xu, who all took part in the mesocosm experiments; we also grateful to the technical supporting staff, Xianglan Zeng, Wenyan Zhao and Litong Peng.

Author Contributions

X. Liu, Y. Li and Y. Wu contributed equally to this paper for their leading roles in field sampling and writing of the manuscript. D. Hutchins and F. Fu contributed to writing and editing the manuscript. K. Gao, M. Dai and B. Huang initially designed the study and supervised the projects. This study was conceived in discussions between all authors.

Additional Information

Supplementary information accompanies this paper at doi:10.1038/s41598-017-07195-8

Competing Interests: The authors declare that they have no competing interests.

Publisher's note: Springer Nature remains neutral with regard to jurisdictional claims in published maps and institutional affiliations.



Open Access This article is licensed under a Creative Commons Attribution 4.0 International License, which permits use, sharing, adaptation, distribution and reproduction in any medium or format, as long as you give appropriate credit to the original author(s) and the source, provide a link to the Creative Commons license, and indicate if changes were made. The images or other third party material in this article are included in the article's Creative Commons license, unless indicated otherwise in a credit line to the material. If material is not included in the article's Creative Commons license and your intended use is not permitted by statutory regulation or exceeds the permitted use, you will need to obtain permission directly from the copyright holder. To view a copy of this license, visit <http://creativecommons.org/licenses/by/4.0/>.

© The Author(s) 2017